

An Aluminum Ate Base: Its Design, Structure, Function, and Reaction Mechanism

Hiroshi Naka,^{*,†,§,¶} Masanobu Uchiyama,^{*,‡,§,¶} Yotaro Matsumoto,^{§,¶}
Andrew E. H. Wheatley,^{*,‡} Mary McPartlin,[‡] James V. Morey,[‡]
and Yoshinori Kondo[†]

Contribution from the Graduate School of Pharmaceutical Sciences, Tohoku University, Aobayama, Aoba-ku, Sendai 980-8578, Japan, Advanced Elements Chemistry Laboratory, The Institute of Physical and Chemical Research, RIKEN, 2-1 Hirosawa, Wako-shi, Saitama 351-0198, Japan, Department of Chemistry, University of Cambridge, Lensfield Road, Cambridge, CB2 1EW, U.K., "Synthesis and Control," PRESTO, Japan Science and Technology Agency (JST), Japan, and Graduate School of Pharmaceutical Sciences, The University of Tokyo, 7-3-1 Hongo, Bunkyo-ku, Tokyo 113-0033, Japan

Received June 29, 2006; E-mail: naka@mail.pharm.tohoku.ac.jp; uchiyama@mol.f.u-tokyo.ac.jp; aehw2@cam.ac.uk

Abstract: An aluminum ate base, *i*-Bu₃Al(TMP)Li, has been designed and developed for regio- and chemoselective direct generation of functionalized aromatic aluminum compounds. Direct aluminations followed by electrophilic trapping with I₂, Cu/Pd-catalyzed C–C bond formation, or direct oxidation with molecular O₂ proved to be a powerful tool for the preparation of 1,2- or 1,2,3-multisubstituted aromatic compounds. This deprotonative aluminations using *i*-Bu₃Al(TMP)Li was found to be effective in aliphatic chemistry as well, enabling regio- and chemoselective addition of functionalized allylic ethers and carbamates to aliphatic and aromatic aldehydes. A combined multinuclear NMR spectroscopy, X-ray crystallography, and theoretical study showed that the aluminum ate base is a Li/Al bimetallic complex bridged by the nitrogen atom of TMP and the α -carbon of an *i*-Bu ligand and that the Li exclusively serves as a recognition point for electronegative functional groups or coordinative solvents. The mechanism of directed ortho aluminations of functionalized aromatic compounds has been studied by NMR and in situ FT-IR spectroscopy, X-ray analysis, and DFT calculation. It has been found that the reaction proceeds with facile formation of an initial adduct of the base and aromatic, followed by deprotonative formation of the functionalized aromatic aluminum compound. Deprotonation by the TMP ligand rather than the isobutyl ligand was suggested and reasoned by means of spectroscopic and theoretical study. The remarkable regioselectivity of the ortho aluminations reaction was explained by a coordinative approximation effect between the functional groups and the counter Li⁺ ion, enabling stable initial complex formation and creation of a less strained transition state structure.

Introduction

Organoaluminum compounds have been widely used both in industrial and laboratory synthetic chemistry,¹ serving as polymer synthesis catalysts,² Lewis acid reagents,³ and organic synthetic building blocks.⁴ As demonstrated by recent developments,⁵ organoaluminum species have become extremely im-

portant synthetic intermediates in the formation of carbon–carbon and carbon–heteroatom bonds, especially in aliphatic chemistry. Therefore, aromatic aluminum compounds should be potentially attractive as functional materials and synthetic building blocks.⁶ However, aromatic aluminum chemistry has not been well developed, simply because of the poor synthetic availability of these systems. A conventional preparative method for aromatic aluminum compounds has been the transmetalation of aryllithium or aryl Grignard reagents.⁷ This method, however, suffers from the limited compatibility of functional groups on

[†] Tohoku University.

[‡] RIKEN.

[§] PRESTO, JST.

[‡] University of Cambridge.

[¶] The University of Tokyo.

- (1) (a) Mole, T.; Jeffrey, E. A. *Organoaluminum Compounds*; Elsevier: Amsterdam, 1972. (b) Hashimoto, S.; Kitagawa, Y.; Iemura, S.; Yamamoto, H.; Nozaki, H. *Tetrahedron Lett.* **1976**, *30*, 2615–2616. (c) Negishi, E. *J. Organomet. Chem. Libr.* **1976**, *1*, 93–125.
- (2) Boor, J. *Ziegler Natta Catalysts and Polymerizations*; Academic Press: New York, 1979.
- (3) (a) Saito, S. Aluminum in Organic Synthesis. In *Main Group Metals in Organic Synthesis*; Yamamoto, H., Oshima, K., Eds.; Wiley-VCH: Weinheim, Germany, 2004; Vol 1, Chapter 6 and references therein. (b) Taylor, M. S.; Zalatan, D. N.; Lerchner, A. M.; Jacobsen, E. N. *J. Am. Chem. Soc.* **2005**, *127*, 1313–1317. (c) Wieland, L. C.; Deng, H.; Snapper, M. L.; Hoveyda, A. H. *J. Am. Chem. Soc.* **2005**, *127*, 15453–15456.

- (4) (a) Nagata, W.; Yoshioka, M.; Hirai, S. *J. Am. Chem. Soc.* **1972**, *94*, 4635–4643. (b) Chen, E. Y.-X.; Cooney, M. J. *J. Am. Chem. Soc.* **2003**, *125*, 7150–7151. (c) Maruoka, K.; Sano, H.; Shinoda, K.; Yamamoto, H. *Chem. Lett.* **1987**, 73–76. (d) Kabalka, G. W.; Newton, R. J., Jr. *J. Organomet. Chem.* **1978**, *156*, 65–69.
- (5) (a) Liang, B.; Novak, T.; Tan, Z.; Negishi, E.-i. *J. Am. Chem. Soc.* **2006**, *128*, 2770–2771. (b) Novak, T.; Tan, Z.; Liang, B.; Negishi, E.-i. *J. Am. Chem. Soc.* **2005**, *127*, 2838–2839.
- (6) Ishikawa, T.; Ogawa, A.; Hirao, T. *J. Am. Chem. Soc.* **1998**, *120*, 5124–5125.
- (7) Eisch, J. J. In *Comprehensive Organometallic Chemistry*; Wilkinson, G., Stone, F. G. A., Abel, E. W., Eds.; Pergamon Press: Oxford, 1982; Vol 6, Chapter 6 and references therein.

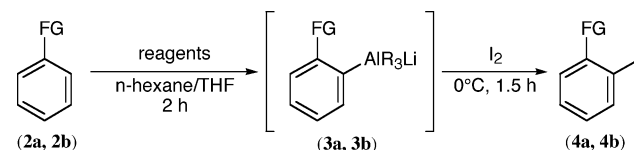
aromatic rings with intermediary ArLi or ArMgX species, or their precursors (alkyllithiums or alkyl Grignard reagents), which are too highly reactive toward various electronegative functional groups, such as halogen, amide, and cyano groups and π -deficient heterocycles.⁸ Hydro- or carbo-alumination, which is known to be a powerful preparative method in aliphatic chemistry,⁹ is ineffective for aromatics because of the structural limitations of benzene rings.¹⁰

To overcome the preparative limitation of aromatic aluminums discussed above, we recently reported that the direct regio- and chemoselective generation of functionalized aromatic aluminum compounds was achieved by developing a novel aluminum ate base *i*-Bu₃Al(TMP)Li (**1**).¹¹ In this article, we will give a full account of the design, structure, function, and reaction mechanism of this aluminum ate base. First we detail its development and discuss its scope and limitations for the generation of functionalized aromatic and aliphatic compounds. Next we characterize the structure of the aluminum ate base using spectroscopic and theoretical methods. Finally we provide a comprehensive mechanistic discussion of the directed ortho alumination of functionalized aromatics by means of X-ray, NMR, IR, and DFT studies.

Results and Discussion

1. Development of the Aluminum Ate Base. To find ideal alumination reagents with broad functional group compatibilities, we first tested the halogen–aluminum exchange reactions of aryl halides using various kinds of organoaluminum reagents.¹² While related alkyllithiums,¹³ alkylmagnesiums,¹⁴ and zincates¹⁵ have been known to effect halogen–metal exchange reactions smoothly, all attempts using organoaluminums were unsuccessful, in spite of extensive investigation. We then employed a different strategy; the deprotonative alumination (i.e., hydrogen–aluminum exchange reaction) of functionalized benzenes. Starting from cleaving an aromatic C–H bond, this reaction would be more advantageous from the viewpoint of the availability of aromatic precursors. Pioneering work on the deprotonation of aliphatic C–H groups using tricoordinated dialkylamidoaluminums has been reported.¹⁶ These reagents, however, were found to be ineffective for our purpose. Therefore, we designed a tetracoordinated aluminum ate base, which should have higher reactivity over conventional tricoordinated aluminums.¹⁷ We first screened ligand and counter cation candidates. Anisole (**2a**) and benzonitrile (**2b**) were selected as model aromatic compounds with electron-donating and electron-withdrawing groups, respectively (Table 1).

Table 1. Ligand Screenings of the Aluminum Ate Base R₃Al(TMP)Li for Direct Generation of Functionalized Aromatic Aluminum Compounds^a



entry	Ph-FG	reagents ^b	product	yield (%) ^c
1	2a (PhOMe)	Me ₃ Al(TMP)Li (1a)	4a	12
2	2a	Et ₃ Al(TMP)Li	4a	87
3	2a	<i>i</i> -Bu ₃ Al(TMP)Li (1)	4a	88
4	2b (PhCN)	Me ₃ Al(TMP)Li (1a)	4b	0
5	2b	Et ₃ Al(TMP)Li	4b	0
6	2b	<i>t</i> -Bu ₃ Al(TMP)Li	4b	0
7	2b	<i>i</i> -Bu ₃ Al(TMP)Li (1)	4b	100

^a Reaction temperatures for the first step of the reaction are room temperature for **2a** and -78 °C for **2b**. ^b TMP = 2,2,6,6-tetramethylpiperidido. ^c Isolated yield.

To our delight, deprotonation with Me₃Al(TMP)Li (**1a**) of **2a** gave the corresponding iodinated compound **4a** in 12% yield after the iodine quench (entry 1). Use of Et₃Al(TMP)Li (entry 2) and *i*-Bu₃Al(TMP)Li (**1**) (entry 3) improved the system dramatically, furnishing **4a** in high yields. In contrast, deprotonative alumination of **2b** suffered from significant decomposition of the CN group when R₃Al(TMP)Li (R = Me, Et, *t*-Bu) was used (entries 4–6). Surprisingly, the only exception to this rule was *i*-Bu₃Al(TMP)Li (**1**), which gave 2-iodobenzonitrile (**4b**) in excellent yield (entry 7). In the deprotonative alumination of **2b**, modification of the *i*-Bu group in **1** to alkoxides or amides, of TMP to N(*i*-Pr)₂ or N(TMS)₂, or of Li to K, MgCl, Mg(*t*-Bu), or Zn(*t*-Bu) also gave a complex mixture of products. Solvent effects have also been tested for the alumination of **2b** with **1**, and use of noncoordinative solvents such as hexane, toluene or CH₂Cl₂, or lower-coordinative ethers resulted in decreased yields. As we found **1** in THF to be a promising chemoselective base, we next explored its reactivity with variously functionalized aromatic compounds (Table 2). In the following discussions, we define *i*-Bu₃Al(TMP)Li (**1**) as aluminum ate base.

The aluminum ate base (**1**) was found to be an effective and regioselective alumination reagent for a variety of (fused) aromatic compounds bearing electron-donating groups such as OMe and electron-withdrawing groups such as CN, amide, Cl, and I (entries 1–12 in Table 2). Notably, deprotonative alumination occurred with suppression of nucleophilic addition to carbonyl and CN groups (entries 2, 3, and 5) or benzyne formation with halogens (entries 4–6, 11, 12) and halogen–metal exchange reaction at iodine (entries 4–6). Such chemoselectivity is considered to be unique to this aluminum ate base, because neither conventional metal bases (such as RLi) nor even TMP zincates can coexist with the aryl iodide.¹⁸ Heteroaromatics such as pyridine, indole, benzofuran, and benzoxazole rings were similarly applicable substrates (entries 13–16). Trifluoromethylbenzene and ferrocenyl esters also tolerated alumination.

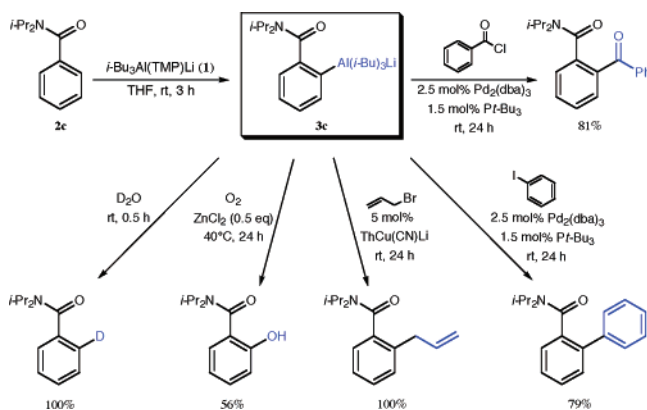
- (8) Upton, C. J.; Beak, P. *J. Org. Chem.* **1975**, *40*, 1094–1098.
 (9) (a) Van Horn, D. E.; Negishi, E.-i. *J. Am. Chem. Soc.* **1972**, *94*, 4654–4672. (b) Eisch, J. J. In *Comprehensive Organic Synthesis*; Trost, B. M., Ed.; Pergamon Press: Oxford, 1991; Vol 8, Chapter 3.
 (10) Hart, H. In *The Chemistry of Triple-Bonded Functional Groups, Supplement C2*; Patai, S., Ed.; John Wiley & Sons Ltd: Chichester, U.K., 1994; Chapter 18.
 (11) Uchiyama, M.; Naka, H.; Matsumoto, Y.; Ohwada, T. *J. Am. Chem. Soc.* **2004**, *126*, 10526–10527.
 (12) For an exceptional example of halogen–aluminum exchange reactions, see: Maruoka, M.; Fukutani, Y.; Yamamoto, H. *J. Org. Chem.* **1985**, *50*, 4412–4414.
 (13) Clayden, J. *Organolithiums: Selectivity for Synthesis*; Pergamon: Elsevier Science, Oxford, 2002.
 (14) Boudier, A.; Bromm, L. O.; Lotz, M.; Knochel, P. *Angew. Chem., Int. Ed.* **2000**, *39*, 4414–4435.
 (15) (a) Uchiyama, M.; Koike, M.; Kameda, M.; Kondo, Y.; Sakamoto, T. *J. Am. Chem. Soc.* **1996**, *118*, 8733–8734. (b) Uchiyama, M.; Kameda, M.; Mishima, O.; Yokoyama, N.; Koike, M.; Kondo, Y.; Sakamoto, T. *J. Am. Chem. Soc.* **1998**, *120*, 4934–4946.

- (16) Yasuda, A.; Tanaka, S.; Oshima, K.; Yamamoto, H.; Nozaki, H. *J. Am. Chem. Soc.* **1974**, *96*, 6513–6514.
 (17) (a) Boireau, G.; Abenhaim, D.; Bernardon, C.; Henry-Basch, E.; Sabourault, B. *Tetrahedron Lett.* **1975**, *16*, 2521–2524. (b) Yamamoto, Y.; Yatagai, H.; Maruyama, K. *J. Am. Chem. Soc.* **1981**, *103*, 1969–1975. (c) Sasaki, M.; Tanino, K.; Miyashita, M. *Org. Lett.* **2001**, *3*, 1765–1767.

Table 2. Deprotonative Almination of Functionalized Aromatic Rings^a

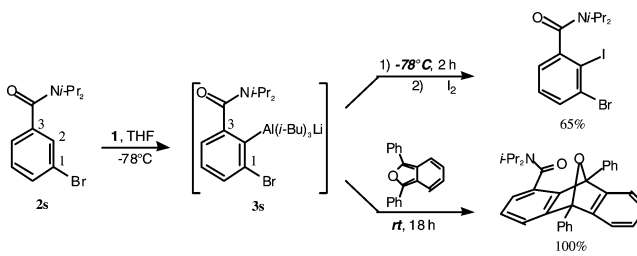
entry	substrate	product	yield (%) ^b	entry	substrate	product	yield (%) ^b	entry	substrate	product	yield (%) ^b
1			99 (rt, 3 h)	7			92 (0°C, 4 h)	13			82 (-78°C, 1 h)
2			100 (-78°C, 2 h)	8			74 (0°C, 4 h)	14			64 (100) ^c (-78°C, 5 h)
3			94 (rt, 3 h)	9			68 (rt, 3 h)	15			88 (rt, 2 h)
4			83 (rt, 3 h)	10			84 (rt, 3 h)	16			86 (0°C, 2 h)
5			90 (-78°C, 2 h)	11			74 (-78°C, 12 h)	17			40 (0°C, 7 h)
6			100 (-78°C, 3 h)	12			72 (-78°C, 5 h)	18			37 (-78°C, 2 h)

^a Unless otherwise noted, the deprotonative almination was carried out using *i*-Bu₃Al(TMP)Li (2.2 equiv) and substrate (1.0 equiv) in THF. ^b Isolated yield. Items in parentheses are conditions of metalation. ^c Value in parentheses is the yield of the 2-deuterate (quenched with D₂O).

Scheme 1. Electrophilic Trapping of the Functionalized Aryl Aluminate Intermediate (**3c**)

Having established a general preparative method for functionalized aromatic aluminum compounds, we next demonstrated that the functionalized aryl aluminate intermediate **3c** (as a typical intermediate) can be utilized as an aryl anion equivalent (Scheme 1).

Intermediate **3c**, generated by the deprotonative almination of **2c** using *i*-Bu₃Al(TMP)Li (**1**), was treated with D₂O to give the corresponding *o*-deuterated product in quantitative yield. When the intermediate **3c** was exposed to molecular oxygen in the presence of 0.5 equiv of ZnCl₂, the corresponding phenol was obtained in 56% yield, realizing the regioselective introduction of an OH group. Since regio- and chemoselective direct introduction of a hydroxyl group onto an aromatic ring is generally difficult, the present procedure should provide a new,

Scheme 2. Thermally Controlled Generation and Suppression of 3-Functionalized Benzynes

convenient one-pot synthesis of functionalized phenols.¹⁹ Intermediate **3c** also undergoes copper- and palladium-catalyzed C–C bond-forming reactions such as allylation, phenylation, and benzylation in high yields and with high chemo- and regioselectivities.

Recently, we reported that the chemo- and regioselective zincation of meta-functionalized haloaromatics and the generation of 3-substituted benzyne could be controlled by utilizing the drastic ligand effects seen in these zincates.²⁰ In the case of the aluminum ate base, generation of benzyne could be controlled by changing the reaction temperature (Scheme 2).

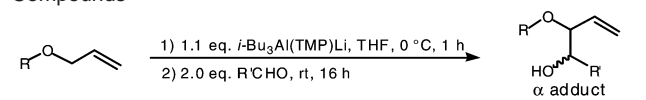
The intermediate **3s**, generated by the deprotonative almination of *N,N*-diisopropyl-3-bromo-2-iodobenzamide (**2s**), could be trapped with an electrophile (I₂) at low temperature, while the generation of a 3-functionalized benzyne proceeded smoothly at room temperature, and this reacted with 1,3-diphenylisobenzofuran to give the corresponding Diels–Alder adduct in quantitative yield.

As the aluminum ate base **1** proved to be an excellent direct almination reagent for functionalized aromatics, we next

(18) (a) Kondo, Y.; Shilai, M.; Uchiyama, M.; Sakamoto, T. *J. Am. Chem. Soc.* **1999**, *121*, 3539–3540. (b) Xu, C.; Yamada, H.; Wakamiya, A.; Yamaguchi, S.; Tamao, K. *Macromolecules* **2004**, *37*, 8978–8983. (c) Uchiyama, M.; Matsumoto, Y.; Usui, S.; Hashimoto, Y.; Morokuma, K. *Angew. Chem., Int. Ed.* **2007**, *46*, 926–929. (d) Mulvey, R. E.; Mongin, F.; Uchiyama, M.; Kondo, Y. *Angew. Chem., Int. Ed.* **2007**, *46*, in press (DOI: 10.1002/anie.200604369).

(19) (a) Maleczka, R. E., Jr.; Shi, F.; Holmes, D.; Smith, M. R., III. *J. Am. Chem. Soc.* **2003**, *125*, 7792–7793. (b) Ishiyama, T.; Takagi, J.; Ishida, K.; Miyaura, N.; Anastasi, N. R.; Hartwig, J. F. *J. Am. Chem. Soc.* **2002**, *124*, 390–391.

(20) Uchiyama, M.; Miyoshi, T.; Kajihara, Y.; Sakamoto, T.; Otani, Y.; Ohwada, T.; Kondo, Y. *J. Am. Chem. Soc.* **2002**, *124*, 8514–8515.

Table 3. Deprotonative Almination of Functionalized Allylic Compounds


entry	substrate	R'	product	yield (%) ^a	α : γ
1		<i>n</i> -Bu		97	99>:<1
2		Ph		77	97:3
3		<i>n</i> -Bu		70	99>:<1
4		Ph		96	85:15
5		Ph		63	79:21
6		Ph		82	99>:<1

^a Isolated yield. Diastereomeric ratio of α -products (erythro/threo); entry 1 (87:13), entry 2 (56:44), entry 3 (not determined), entry 4 (82:17), entry 5 (58:42), entry 6 (99:1). *E/Z* ratios of γ -products were not determined.

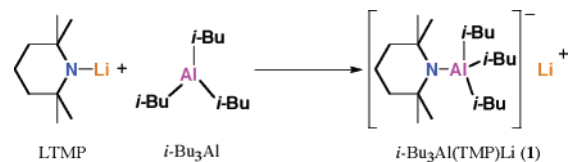
extended its scope to functionalized aliphatic compounds. Various oxygen-substituted allylic species were chosen for substrates because of their easy accessibility and their potential transformability.²¹ For instance, allylcarbamates are attractive substrates as they can be easily converted to π -allylpalladium species.²² A conventional direct preparative method of an allylic anion intermediate requires deprotonation using reactive alkali metal species such as alkyllithiums and involves low functional group compatibilities and inefficient α/γ regioselectivity.²³ Transmetalation of these allylic alkali metals with Et₃Al to give allylic aluminates, or with Bu₃SnCl to give allylic tin compounds, improved the regioselectivity dramatically, reaction with aldehydes occurring at the α position.²⁴ However, this stepwise strategy needs strictly controlled reaction conditions in the first deprotonation step. Moreover, it has been difficult to apply to allylic compounds with reactive functional groups, such as carbonyl or phenoxy groups, because the highly reactive alkyllithium reagents or intermediary allylmetal species cause S_N2 or S_N2' decomposition of allylic substrates or products.²⁵ Therefore, a direct preparative route to a functionalized allylic anion equivalent under mild conditions via successive regioselective transformations is highly desirable. We found that this could be achieved by direct generation of the functionalized allylic aluminum compounds using **1** as base, realizing the one-pot regioselective transformation under mild conditions (Table 3).

The deprotonative almination of oxygen-substituted allylic compounds by **1** was found to be regioselective and tolerant of

ethers and carbamates under mild conditions. When MOM ether was used, high regioselectivity was accomplished to furnish **6a** (quenched with *n*-BuCHO) and **7a** (quenched with PhCHO) in good yields (entries 1 and 2). Compound **1** also reacted chemoselectively with allylcarbamates to give α -substituted allylic compounds in moderate to excellent yields (entries 3–5). Sequential almination and electrophilic trapping of allyl-(2-methoxyphenyl)ether **5d** was found to be highly regio- and stereoselective (entry 6). As this selectivity was not observed in unsubstituted allylphenylether, it is possible that the methoxy group works as an optional directing group for the counter Li⁺ cation, fixing the relative position and direction of the aldehyde with respect to the allylaluminate.

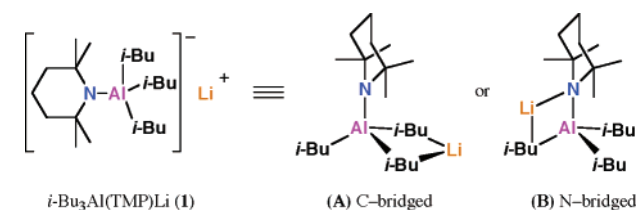
Summarizing this section, aluminum ate base **1** has been found to effect the deprotonative almination of functionalized aromatic, heteroaromatic, and allylic compounds with exceptionally high chemo- and regioselectivity. In the coming sections, aiming to obtain suggestions for improving reactivity and selectivity of the current system and to achieve the logical design of more efficient reagents, a structural study of *i*-Bu₃Al(TMP)-Li (**1**) and a mechanistic investigation of its almination reactions are discussed in detail.

2. Structural Study of the Aluminum Ate Base. The developed aluminum ate base *i*-Bu₃Al(TMP)Li (**1**) can be prepared simply by mixing *i*-Bu₃Al and LTMP in a 1:1 ratio in THF, and one would expect the lithium aluminum ate structure of **1** to be that shown in Scheme 3.²⁶

Scheme 3

We first studied THF solutions of **1**, *i*-Bu₃Al and LTMP by ¹H, ¹³C, ⁷Li, ¹⁵N, and ²⁷Al NMR spectroscopy at -50 °C (Table 4).

The aluminum ate base **1** has been observed as a novel *single* species in THF solution. No signals corresponding to *i*-Bu₃Al or LTMP were detected.³² The ²⁷Al chemical shift (153.4 ppm) of **1** showed clean formation of a tetrahedrally disposed aluminum center, indicating strong coordination of the nitrogen of the TMP ligand to the aluminum. These results confirmed clean and complete formation of the “ate” complex **1** as shown in Scheme 3. However, since the three isobutyl groups of **1** were identical on the NMR time scale, the issue left for complete structural determination was to understand the relative positions of Li⁺ ion and the other fragments (Figure 1).

**Figure 1.** Two possible isomers of the aluminum ate base **1**.

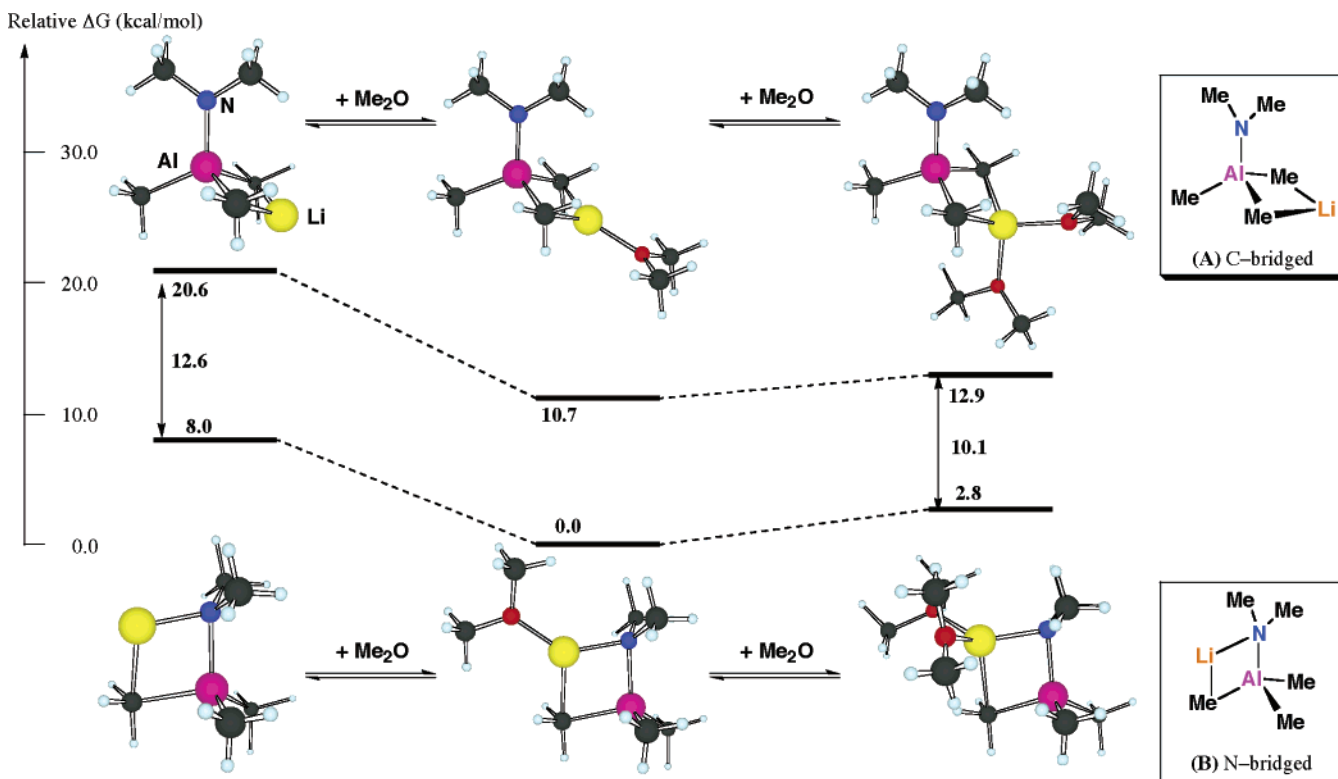
- (21) Yamamoto, Y.; Asao, N. *Chem. Rev.* **1993**, *93*, 2207–2293.
 (22) (a) Guibe, F. *Tetrahedron* **1998**, *54*, 2967–3042. (b) Hoppe, D. *Angew. Chem., Int. Ed.* **1984**, *23*, 932–948.
 (23) Still, W. C.; Macdonald, T. L. *J. Am. Chem. Soc.* **1974**, *96*, 5562–5563.
 (24) (a) Yamamoto, Y.; Yatagi, H.; Saito, Y.; Maruyama, K. *J. Org. Chem.* **1984**, *49*, 1096–1104. (b) Yamamoto, Y. *Acc. Chem. Res.* **1987**, *20*, 243–249. (c) Kadota, I.; Yamamoto, Y. *Acc. Chem. Res.* **2005**, *38*, 423–432.
 (25) In situ generation of allylmetal species from allylhalides represents an alternative approach, though the accessibility of functionalized precursors is a concern. See: Kurosu, M.; Lin, M.-H.; Kishi, Y. *J. Am. Chem. Soc.* **2004**, *126*, 12248–12249.

- (26) Wittig, G. *Q. Rev.* **1996**, 191–210.

Table 4. ^1H , ^{13}C , ^7Li , ^{15}N , and ^{27}Al NMR Spectroscopic Data for THF Solutions of LTMP, $i\text{-Bu}_3\text{Al}$, and $i\text{-Bu}_3\text{Al}(\text{TMP})\text{Li}$ (**1**)^a

	^1H	^{13}C	^7Li	^{15}N	^{27}Al
$i\text{-Bu}_3\text{Al}$	−0.16 (d, 6H), 1.72 (m, 3H) 0.85 (m, 18H)	23.4 (α), 27.8 (β) 29.1 (γ)			174.4
LTMP	1.06 (s, 12H), 1.15 (4H) 1.56 (m, 2H)	20.9 (γ), 36.2 (Me) 43.3 (β), 53.1 (α)	0.61 (monomer) 1.26 (dimer)	79.9	
$i\text{-Bu}_3\text{Al}(\text{TMP})\text{Li}$	0.98 (s, 12H), 1.20 (4H) 1.54 (m, 2H) −0.47 (6H), 1.69 (m, 3H) 0.77 (m, 18H)	19.3 (TMP $^\gamma$), 32.3 (TMP ^{Me}) 39.0 (TMP $^\beta$), 50.1 (TMP $^\alpha$) 24.4 ($i\text{-Bu}^\alpha$), 30.2 ($i\text{-Bu}^\beta$) 29.4 ($i\text{-Bu}^\gamma$)	−0.75	77.0	153.4

^a Reported NMR data for $i\text{-Bu}_3\text{Al}$ (δ (ppm) $\alpha\text{-H}$ (0.30), $\beta\text{-H}$ (1.94), $\gamma\text{-H}$ (0.98) in benzene- d_6 (ref 27), ^{27}Al (276) in toluene- d_8 (ref 28)) and LTMP (δ (ppm) $\alpha\text{-C}$ (53.1), $\beta\text{-C}$ (43.1), $\gamma\text{-C}$ (20.9), Me (36.3), ^7Li (0.7 (monomer)) and (1.3 (dimer)), ^{15}N (79.7) in THF- d_8) (refs 29–31).

**Figure 2.** Stationary points of carbon-bridged structure **A** and nitrogen-bridged structure **B** for non-, mono-, and disolvated states at the B3LYP/6-31+G* level with zero-point corrections and entropy term corrections. Free energies given are in kcal/mol and are relative to the monosolvated structure of **B**.

Two structural isomers are possible: Li^+ connected to two alkyl groups (**A**) or to TMP and one alkyl group (**B**). To decide which is more likely, we compared the relative energies of these isomers using computational methods (Figure 2).

We first used a theoretical model of $\text{Me}_3\text{Al}(\text{Me}_2\text{N})\text{Li}$ for **1** and Me_2O for solvent THF. Non-, mono-, and disolvated states of **A** and **B** were considered. The structure **B** was found to be more favorable than **A** by 10–13 kcal/mol at the B3LYP/6-31+G* level of theory, irrespective of the solvation numbers, with monosolvated **B** found to be of lowest in energy.³³

Table 5. ^1H , ^{13}C , ^7Li , ^{15}N , and ^{27}Al NMR GIAO-Predicted Data of $i\text{-Bu}_3\text{Al}(\text{TMP})\text{Li}$ (**1**)^a

	^1H	^{13}C	^7Li	^{15}N	^{27}Al
	1.16 (12H), 1.27 (4H)	18.5 (TMP $^\gamma$), 30.5 (TMP ^{Me})	−2.30	80.5	141.0
	1.61 (2H)	45.1 (TMP $^\beta$), 56.3 (TMP $^\alpha$)			
	−0.15 (6H), 1.87 (3H)	28.7 ($i\text{-Bu}^\alpha$), 30.8 ($i\text{-Bu}^\beta$)			
	0.90 (18H)	25.7 ($i\text{-Bu}^\gamma$)			

^a Mono-(Me_2O)- $i\text{-Bu}_3\text{Al}(\text{TMP})\text{Li}$ has been optimized at the B3LYP/6-31+G* level of theory. GIAO values were calculated at the B3LYP/6-311+G* level of theory and referenced to THF (^1H , ^{13}C), LiBr (^7Li), aniline (^{15}N), and $\text{Al}(\text{NO}_3)_3$ (^{27}Al). Values of equivalent protons and carbons were averaged.

(27) Sen, B.; White, G. L. *J. Inorg. Nucl. Chem.* **1973**, *35*, 2207–2215.

(28) Benn, R.; Rufinska, A.; Lehmkuhl, H.; Janssen, E.; Kturrhrt, C. *Angew. Chem., Int. Ed.* **1983**, *22*, 779–780.

(29) Hall, P. L.; Gilchrist, J. H.; Harrison, A. T.; Fuller, D. J.; Collum, D. B. *J. Am. Chem. Soc.* **1991**, *113*, 9575–9585.

(30) Renaud, P.; Fox, M. A. *J. Am. Chem. Soc.* **1988**, *110*, 5702–5705.

(31) Romesberg, F. E.; Gilchrist, J. H.; Harrison, A. T.; Fuller, D. J.; Collum, D. B. *J. Am. Chem. Soc.* **1991**, *113*, 9575–9577.

(32) See the SI for each NMR chart.

(33) ^{27}Al NMR GIAO calculation for these structures also supported this view.

^{27}Al NMR GIAO calculation at the level of B3LYP/6-311+G*/B3LYP/6-31+G* (values in ppm and referenced to $\text{Al}(\text{NO}_3)_3$): **A**, 135.15; **A-Me₂O**, 134.67; **A-2Me₂O**, 133.33; **B**, 155.97; **B-Me₂O**, 154.22; **B-2Me₂O**, 153.71. Experimental value: 153.4 ppm.

Next, we conducted full optimizations of $i\text{-Bu}_3\text{Al}(\text{TMP})\text{Li}$ with 0, 1, or 2 Me_2O solvent molecules using the same level of theory. In harmony with the $\text{Me}_3\text{Al}(\text{Me}_2\text{N})\text{Li}$ model, the monosolvated structure has been found to be most stable, and the GIAO-predicted chemical shifts of this monosolvated $i\text{-Bu}_3\text{Al}(\text{TMP})\text{Li}$ showed good agreement with the experimental values (Tables 4 and 5).

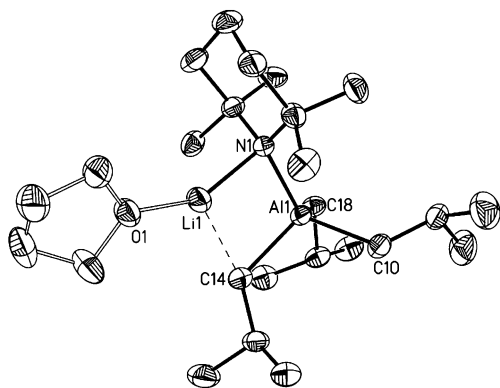


Figure 3. Molecular structure of **1**–THF. Hydrogen atoms are omitted for clarity. Atoms are plotted at 40% probability.

Finally, we have obtained X-ray crystallographic evidence for the structure of *i*-Bu₃Al(TMP)Li (**1**)–THF complex (Figure 3).

The sequential treatment of HTMP with *n*-BuLi and *i*-Bu₃Al in THF afforded crystalline **1**–THF. Its structure reveals that the lithium ion acts as an exclusive recognition point for electron-rich donors. Notably, the essential structure observed revealed a core Li–N–Al–C metalocycle³⁴ with a bridging TMP and single bridging *i*-Bu ligand (Li1–N1 1.985(4), Li1–C14 2.258(4), Al1–N1 1.9900(16), Al1–C14 2.067(2) Å).³⁵ The similarity borne by the solid-state structure of **1**–THF to the calculated structure of monosolvated **B** is striking, and strongly suggests the validity of our NMR spectroscopic and computational analysis.

On the basis of this experimental and theoretical evidence, we have concluded that the aluminum ate base is likely to be a Li/Al bimetallic complex, bridged by the nitrogen atom of TMP

and the α -carbon of a single *i*-Bu group, with the counter Li⁺ ion exclusively serving as a recognition point for coordinative solvents and/or electronegative functional groups.

3. Mechanism of Directed ortho Almination of Functionalized Aromatic Compounds. Having obtained the structure of the aluminum ate base that is likely to be experimentally relevant, we next investigated the reaction mechanism of directed ortho almination in detail.

3.1. Characterization of Aluminated Aromatic Compounds. To obtain direct spectroscopic evidence for the formation of the aluminated arene intermediates, we monitored reactions using ¹³C NMR spectroscopy (Figure 4).

Anisole (**2a**) was chosen as aromatic substrate, and we first monitored its stepwise reaction with *t*-BuLi to form ortho-lithiated anisole (**3a'**) and then with *i*-Bu₃Al to give ortho-aluminated compound **3a**. In the first step, the chemical shift for the lithiated ortho carbon moved significantly to low field (from $\delta = 114.3$ ppm (spectrum a) to 163.7 ppm (spectrum b)), revealing the formation of **3a'**. Addition of *i*-Bu₃Al gave ortho-aluminated **3a** with the chemical shift of the ortho carbon at 152.9 ppm (spectrum c). Next we investigated the direct reaction of **2a** with **1**. In spectrum d, each signal for the newly emerged intermediate was found to be identical with that of stepwise-prepared **3a**, with no signals for **3a'** being found. These results clearly showed that the aluminum ate base reacts with **2a** to directly generate ortho-aluminated aryl species **3a**.

3.2. Regioselectivity in Deprotonative Almination. A considerable number of examples of directed ortho metalation have been recorded,³⁶ and their regioselectivities have been generally explained by a complex-induced approximate effect and/or an acidifying inductive effect of the aromatic substituents.³⁷ However, the mechanistic details of directed metalation

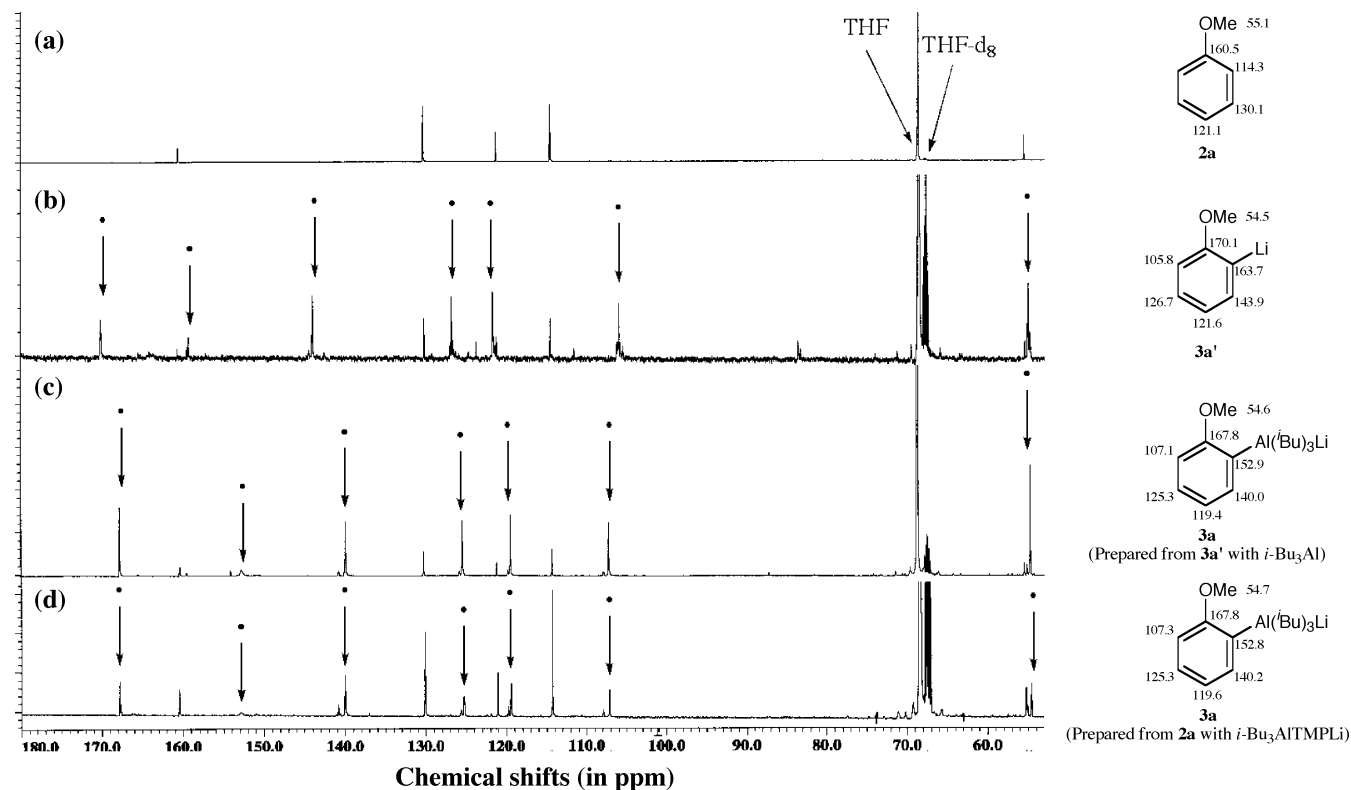


Figure 4. ¹³C NMR spectra of (a) anisole (**2a**) in THF, (b) **2a** + *t*-BuLi, (c) **2a** + *t*-BuLi, then added *i*-Bu₃Al, (d) **2a** + *i*-Bu₃Al(TMP)Li. Signals for 2-lithioanisole (**3a'** in b) and (2-MeOC₆H₄)Al(*i*-Bu)₃Li (**3a** in c, d) are marked with dots.

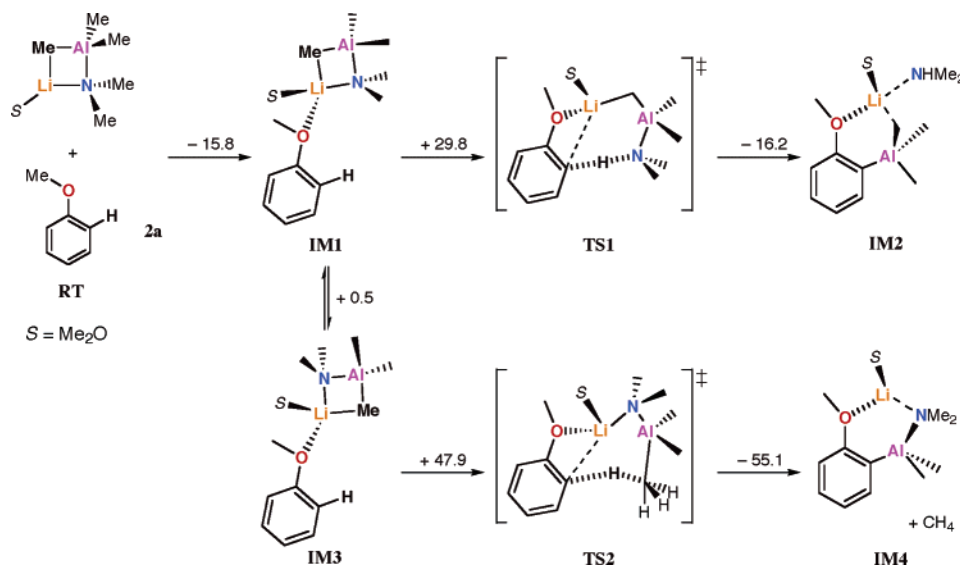


Figure 5. Stationary and transition points during possible deprotonative aluminations of **2a** with $\text{Me}_3\text{Al}(\text{Me}_2\text{N})\text{Li}-\text{OMe}_2$ at the B3LYP/6-31+G* level of theory. Energy changes at B3LYP/6-31+G* level during deprotonation with NMe₂ ligand or Me ligand are shown in kcal/mol.

with ate complexes seem complicated and unclear.³⁸ To shed light on the mechanism of directed ortho aluminations, we investigated the possible pathways using DFT calculations (Figure 5).

We chose **2a** as a model aromatic substrate and $\text{Me}_3\text{Al}(\text{Me}_2\text{N})\text{Li}-\text{OMe}_2$ (monosolvated **B** in Figure 3) as the aluminum ate base on the dual grounds of its relative calculational simplicity and its successful structural characterization.³⁹ Although the choice of this simplified model system may lead to an underestimation of the steric effects of bulky groups (e.g., *i*-Bu), the essence of the actual reaction nature should still be observable using this model system.⁴⁰

Reaction coordinates started with formation of a relatively stable initial complex (**IM1**), with no other pathways (that omitted formation of this intermediate) being found. This theoretical result indicated that the regioselectivity of the ortho aluminations can be explained by a coordinative approximation effect between functional group and Li⁺ ion, enabling initial complex formation and orienting the ate base ligand exclusively toward aromatic ortho hydrogen. To observe an interaction between Li⁺ and the directing functional group on the aromatic substrate in the initial complex, we then used

in situ FT-IR spectroscopy to monitor the aluminations of **2c**, for it possess a C=O group with a strong stretching vibration (Figure 6).

Addition of **2c** to a THF solution of **1** at $-25\text{ }^\circ\text{C}$ gave a transient peak at 1585 cm^{-1} and, along with the disappearance of this peak, a new signal at 1600 cm^{-1} . Elevating the temperature to room temperature did not cause any significant spectral change, and the reaction mixture was quenched with iodine to give 2-iodo-*N,N*-diisopropylbenzamide **4c**. Throughout this process no lithiated aromatic compounds (1578 cm^{-1} in THF)^{18a} were detected. These results suggested that the signal at 1600 cm^{-1} was attributable to the carbonyl group of ortho-aluminated *N,N*-diisopropylbenzamide (**3c**) and that the signal at 1585 cm^{-1} originated from an initial complex between **1** and **2c**, in accordance with theoretical study. As these frequencies are lower than that of the substrate (1636 cm^{-1}), a direct interaction between the carbonyl functional group and the Li⁺ ion in these intermediates can be strongly implied.

To our delight, a snap shot of the type of initial complex indicated by in situ FT-IR spectroscopy was obtained by X-ray crystallographic analysis (Figure 7) of the product of treatment of preisolated **1a** (methyl analogue of **1**) with **2c** in THF.

Two crystallographically independent rotomers are observed in the asymmetric unit of the 1:1 electrostatic adduct **1a-2c**. In either case the lithium ion is in contact with the oxygen atom of the carboxylic amide functional group.⁴¹ The **1a** component possesses a heterobimetallic core, retaining the essential structural features noted for **1-THF**. The major difference between the two adducts lies in the torsional angles observed between carbon-oxygen and lithium-TMP interactions; at C1-O1-Li1-N2 $53.0(10)^\circ$ and C26-O2-Li2-N4 $40.6(13)^\circ$ these suggest some flexibility in the precise arrangement of the two components of either independent adduct. These structural results are in harmony with data obtained from NMR spectroscopy, calculation, and in situ FT-IR observation.

- (34) (a) Niemeyer, M.; Power, P. P. *Organometallics* **1995**, *14*, 5488–5489. (b) Armstrong, D. R.; Craig, F. J.; Kennedy, A. R.; Mulvey, R. E. *Chem. Ber.* **2001**, *129*, 1293–1300. (c) Linton, D. J.; Schooler, P.; Wheatley, A. E. H. *Coord. Chem. Rev.* **2001**, *223*, 53–115. (d) Cui, C.; Schmidt, J. A. R.; Arnold, J. *Dalton Trans.* **2002**, 2992–2994.
- (35) Rutherford, D.; Atwood, D. A. *J. Am. Chem. Soc.* **1996**, *118*, 11535–11540.
- (36) Hartung, C. G.; Snieckus, V. The Directed ortho Metalation Reaction. A Point of Departure for New Synthetic Aromatic Chemistry. In *Modern Arene Chemistry*; Astruc, D., Ed.; Wiley-VCH: New York, 2002.
- (37) (a) Beak, P.; Meyers, A. I. *Acc. Chem. Res.* **1986**, *19*, 356–363. (b) Bauer, W.; Schleyer, P. v. R. *J. Am. Chem. Soc.* **1989**, *111*, 7191–7198. (c) Whisler, M. C.; MacNeil, S.; Snieckus, V.; Beak, P. *Angew. Chem., Int. Ed.* **2004**, *43*, 2206–2225. (d) Rennels, R. A.; Maliakal, A. J.; Collum, D. B. *J. Am. Chem. Soc.* **1998**, *120*, 421–422. (e) Chadwick, S. T.; Rennels, R. A.; Rutherford, J. L.; Collum, D. B. *J. Am. Chem. Soc.* **2000**, *122*, 8640–8647.
- (38) (a) Clegg, W.; Dale, S. H.; Hevia, E.; Harrington, R. W.; Hevia, E.; Honeyman, G. W.; Mulvey, R. E. *Angew. Chem., Int. Ed.* **2006**, *45*, 2370–2374. (b) Clegg, W.; Dale, S. H.; Harrington, R. W.; Hevia, E.; Honeyman, G. W.; Mulvey, R. E. *Angew. Chem., Int. Ed.* **2006**, *45*, 2374–2377.
- (39) A model system without a solvent molecule was also a possible choice, and we confirmed that it provided similar energy values to the presently discussed solvated system.

(40) Both $\text{Me}_3\text{Al}(\text{TMP})\text{Li}$ and $\text{Me}_3\text{Al}(\text{TMP})\text{Li}-\text{THF}$ adopt structures analogous to that of **1-THF**. See the SI for details.

(41) In contrast to recent work on the *N,N*-diisopropylbenzamide adduct of (*t*-Bu)₂Zn(TMP)Li, both rotomers of **1a-(N,N-diisopropylbenzamide)** place the TMP ligand in proximity to the target aryl. See ref 38a.

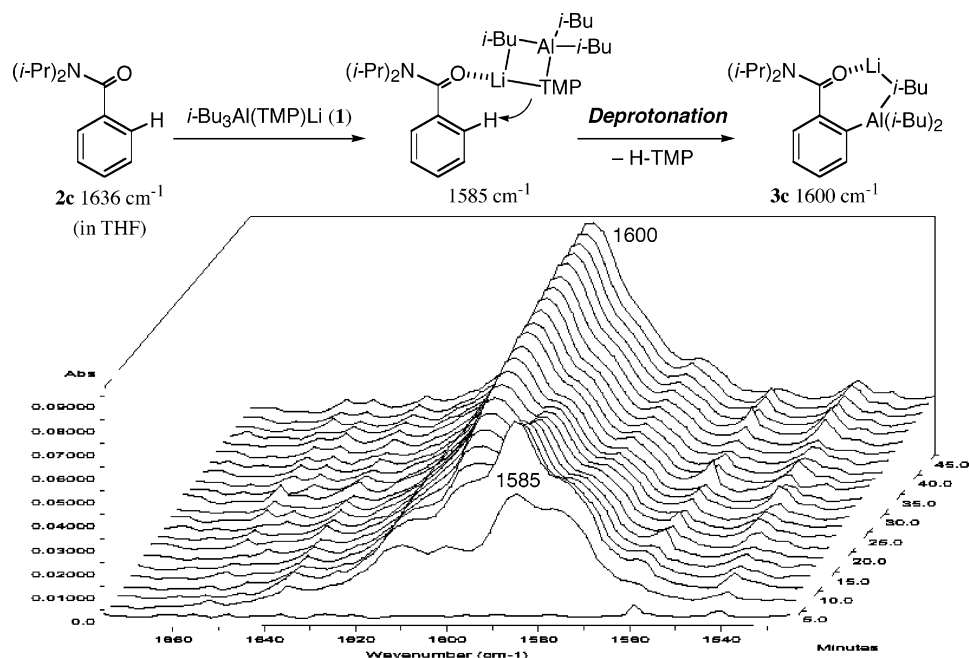


Figure 6. In situ FT-IR monitoring of the deprotonative aluminations of **2c** with **1**.

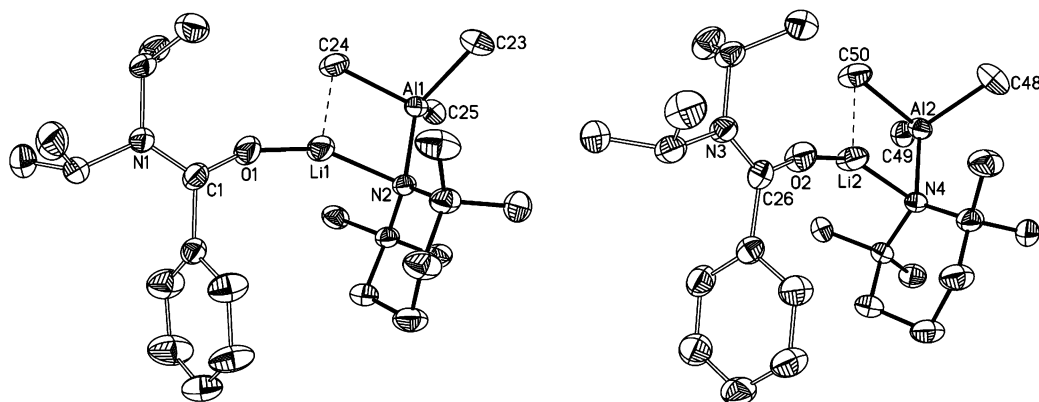


Figure 7. Molecular structure of the two crystallographically independent rotomers of **1a–2c** complex. Hydrogen atoms are omitted for clarity, and atoms are plotted at 40% probability.

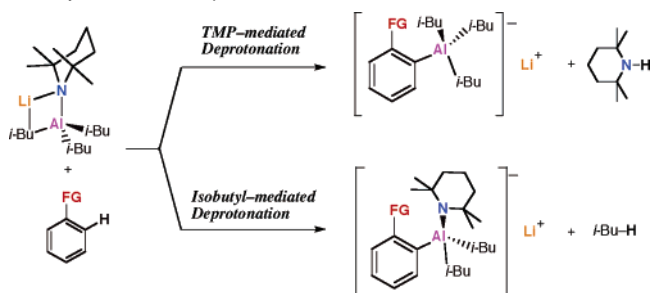
Overall, it was concluded that the remarkable regioselectivity of the ortho aluminations reaction was explicable by there being a coordinative approximation effect between functional group and counter Li^+ ion, enabling stable initial complex formation and a less strained transition structure.

3.3. Ligand Selectivity in Deprotonative Aluminations

Without, as yet, any concrete picture of the reaction pathway in respect of the ligand selectivity shown by the aluminum ate base, we extended our investigation to consider transition states in deprotonation of a functionalized aromatic by the TMP nitrogen ligand and by the isobutyl carbon ligand (Scheme 4).

Because it is well-known that nitrogen ligands are generally more reactive than carbon ligands in mixed ligand aluminum compounds,⁴² TMP-mediated deprotonation is expected to be more plausible than isobutyl-mediated deprotonation. In the case of related TMP–zincate base, however, this ligand selectivity has been reported to be variable depending on the specifics of the complexes themselves and the reaction conditions.⁴³

Scheme 4. TMP-Mediated Deprotonation versus Isobutyl-Mediated Deprotonation



Of several possible TSs for the deprotonation of anisole using the Me and N ligand on the model aluminate, we identified only two TSs, **TS1** and **TS2** (Figures 5 and 8), that were energetically plausible. From **IM1**, both amido-mediated and

(42) (a) Lipton, M. F.; Basha, A.; Weinreb, S. M. *Organic Synthesis*; Wiley: New York, 1988; Collect Vol VI, pp 492–495. (b) Maruoka, K.; Oishi, M.; Yamamoto, H. *J. Org. Chem.* **1993**, *58*, 7638–7639.

(43) (a) Clegg, W.; Dale, S. H.; Drummond, A. M.; Hevia, E.; Honeyman, G. W.; Mulvey, R. E. *J. Am. Chem. Soc.* **2006**, *128*, 7434–7435. (b) Armstrong, D. R.; Clegg, W.; Dale, S. H.; Hevia, E.; Hogg, L. M.; Honeyman, G. W.; Mulvey, R. E. *Angew. Chem., Int. Ed.* **2006**, *45*, 3775–3778. (c) Mulvey, R. E. *Organometallics* **2006**, *25*, 1060–1075. (d) Uchiyama, M.; Matsumoto, Y.; Nobuto, D.; Furuyama, T.; Yamaguchi, K.; Morokuma, K. *J. Am. Chem. Soc.* **2006**, *128*, 8748–8750.

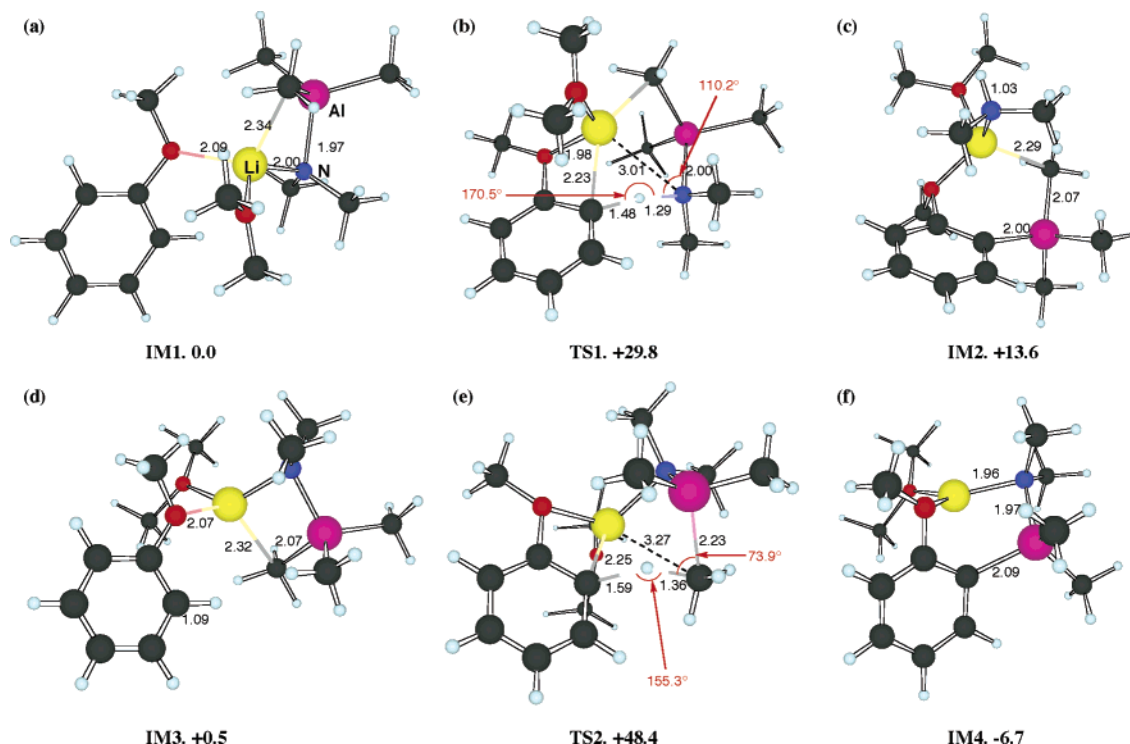


Figure 8. Stationary and transition structures during possible deprotonative aluminations of **2a** at the B3LYP/6-31+G* level of theory. Energies are given in kcal/mol and are relative to structure **IM1**. Deprotonation by the nitrogen-centered ligand: (a) **IM1**, (b) **TS1**, (c) **IM2**. Deprotonation by the carbon-centered ligand: (d) **IM3**, (e) **TS2**, (f) **IM4**. Both **TS1** and **TS2** are denoted as “open form” TS, whereas no “closed form” TS had been found in either system (ref 44).

alkyl-mediated paths are found. In the NMe₂-mediated path, dissociation of the nitrogen atom from lithium leads to a transition state structure (**TS1**) with an activation barrier of 29.8 kcal/mol, producing an aluminated aromatic compound, **IM2**. Deprotonation by the Me ligand on Al (**IM3**-**TS2**-**IM4**) was found to be kinetically unfavorable, requiring a much higher activation energy of 47.9 kcal/mol (18.6 kcal/mol higher than NMe₂). These results strongly suggest that deprotonative almination is affected by the TMP ligand rather than by the *i*-Bu ligand, which is reasonably consistent with recent reported work on TMP zincate.^{43d}

Analysis of local structure of the mediating ligand in either TS (Figure 8) and of the orbital(s) involved in C_{ortho}-H scission (Figure 9) provided a key to understanding this remarkable ligand transfer selectivity.

In **TS1**, the nitrogen atom in the NMe₂ ligand has a relaxed tetrahedral structure, allowing optimal interaction of the nitrogen lone pair with an ortho-hydrogen (Al-N-H angle, 110.2°; N-H-C_{ortho} angle, 170.5°). In the orbital analysis, therefore, an efficient linear orbital overlap between the lone pair of nitrogen and the unoccupied aromatic σ_{C-H}^* orbital is observed, allowing an early transition state (C_{ortho}-H, 1.48 Å) with lower activation energy for the NMe₂-mediated deprotonation pathway. In the case of deprotonation by the Me ligand (**TS2**), however, the bridging carbon atom reveals an unfavorable five-coordinate distorted geometry (Al-C_{Me}-H angle, 73.9°; C_{Me}-H-C_{ortho}

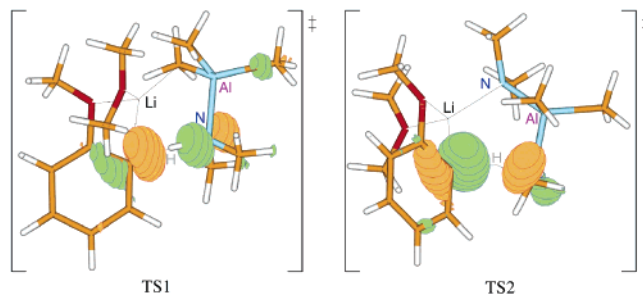


Figure 9. Kohn-Sham highest occupied molecular orbital (HOMO) of **TS1** and **TS2** (ref 45).

angle, 155.3°). Here, the unoccupied aromatic σ_{C-H}^* orbital needs to interact with the contracted and ill directed sp³-like orbital of the carbon atom, resulting in a late transition state (C_{ortho}-H, 1.59 Å) with a higher activation barrier.

In accordance with the direct ¹³C NMR spectroscopic observation of TMP-mediated deprotonation product **3a**, we concluded, with theoretical justification, that the deprotonation of functionalized arenes with aluminum ate base takes place by virtue of the TMP ligand rather than the isobutyl ligand.

3.4. Summary of Mechanism in Directed ortho Almination. On the basis of experimental and theoretical evidence, it can be suggested that aluminum ate base **1** deprotonates functionalized aromatic compounds *directly*, to generate functionalized aromatic aluminum compounds. Observation of the initial 1:1 electrostatic complex, in which Lewis acidic Li⁺ interacts with the functional group of the arene, provided a mechanistic insight into regioselectivity of this novel directed ortho almination. Concerning ligand transfer selectivity of the aluminum ate base, deprotonation by TMP rather than by an isobutyl group is preferred.

(44) Excellent ideas and methods to generate the “open form” TS in organolithium (lithium homobimetal) chemistry have been reported, for example: (a) Zhao, P.; Collum, D. B. *J. Am. Chem. Soc.* **2003**, *125*, 4008–4009. (b) Zhao, P.; Collum, D. B. *J. Am. Chem. Soc.* **2003**, *125*, 14411–14424. (c) Zhao, P.; Condo, A.; Keresztes, I.; Collum, D. B. *J. Am. Chem. Soc.* **2004**, *126*, 3113–3118. (d) Qu, B.; Collum, D. B. *J. Am. Chem. Soc.* **2005**, *127*, 10820–10821.

(45) Kohn, W.; Sham, L. *J. Phys. Rev.* **1965**, *140*, A1133–A1138.

Conclusion

The aluminum ate base, *i*-Bu₃Al(TMP)Li, has been developed as a novel base reagent, realizing highly chemo- and regioselective deprotonative aluminations of functionalized aromatic and heteroaromatic compounds, as well as functionalized allylic compounds. This simple and straightforward method will provide direct and efficient access to valuable synthetic intermediates.

Full structural characterization of *i*-Bu₃Al(TMP)Li and a detailed mechanistic investigation of its role in directed ortho almination have been conducted by means of NMR spectroscopy, in situ FT-IR spectroscopic monitoring, and X-ray crystallographic and theoretical methods, and the origins of the remarkable regioselectivity and ligand transfer selectivity observed have been elucidated. With the comprehensive structural and mechanistic knowledge acquired during this research, improvement of the reaction system and the logical design of

new chemoselective base reagents are in progress in our laboratory. Furthermore, in conjunction with our recent investigations,⁴⁶ complete separation and controlled switching of reactivities in nucleophilic addition, deprotonation, halogen–metal exchange, redox, and transmetalation reactions are envisaged.

Acknowledgment. This research was partly supported by the Astellas Foundation, The Sumitomo Foundation, and a Grant-in-Aid for Young Scientists (A), HOUGA, and Priority Area (No. 452) from the Ministry of Education, Culture, Sports, Science and Technology, Japan (to M.U.). This research was also supported by the Exploratory Research Program for Young Scientists (ERYS) (to H.N. and Y.M.). We also gratefully acknowledge the U.K. EPSRC for financial support (M.McP. and J.V.M.). We thank Dr. Robert P. Davies (Imperial College London) for aid with crystallography and Professor T. Ohwada (The University of Tokyo) for his valuable comments.

Supporting Information Available: Details of the experimental procedures, spectral and crystallographic data. This material is available free of charge via the Internet at <http://pubs.acs.org>.

JA064601N

- (46) (a) Uchiyama, M.; Matsumoto, Y.; Nakamura, S.; Ohwada, T.; Kobayashi, N.; Yamashita, N.; Matsumiya, A.; Sakamoto, T. *J. Am. Chem. Soc.* **2004**, *126*, 8755–8759. (b) Kobayashi, M.; Matsumoto, Y.; Uchiyama, M.; Ohwada, T. *Macromolecules* **2004**, *37*, 4339–4341. (c) Uchiyama, M.; Furuyama, T.; Kobayashi, M.; Matsumoto, Y.; Tanaka, K. *J. Am. Chem. Soc.* **2006**, *128*, 8404–8405. (d) Nakamura, S.; Uchiyama, M. *J. Am. Chem. Soc.* **2007**, *129*, 28–29.